EVALUATION OF ALPHA-PHASED ZIRCONIUM PHOSPHATE NANOPARTICLES AS A CLAY STABILIZER AND AN EOR AGENT

A Thesis

by

YI ZHOU

Submitted to the Office of Graduate and Professional Studies of
Texas A&M University
in partial fulfillment of the requirements for the degree of

MASTER OF SCIENCE

Chair of Committee,	Hisham A. Nasr-El-Din
Committee Members,	Mahmoud El-Halwagi
	David Schechter
Head of Department,	A. Daniel Hill

December 2014

Major Subject: Petroleum Engineering

ABSTRACT

Fines migration, which is the detachment and movement of fines from sand surfaces, leads to the plugging of throats in porous media and becomes an important reason for formation damage. Enhanced Oil Recovery (EOR) is the technique to extract more oil after secondary recovery. Nanoparticles are used as clay stabilizers and EOR agent because of their very small size, large surface area, and surface electrical charge. In this paper, an α-ZrP nanoparticle-based treatment is developed to prevent fines migration in sandstone formations and recovery more oil in carbonate.

To test the ability of α-ZrP nanofluids as a clay stabilizer, coreflood tests were conducted using alpha phased zirconium phosphate based nanofluids as a clay stabilizer with Berea sandstone cores (6 in. in length, 1.5 in. in diameter) under a pressure of 1000 psi and temperature of 300°F. In these experiments, α-ZrP nanofluids were injected at concentrations of 0.1, 0.5, and 1.0 wt% at a flow rate of 2 cm^3/min. Both DI water and brine were used as diluting agents. After each treatment, a post-flush of fresh water was applied. The pressure drop across the core was measured, the core effluent samples were collected, and the permeability changes were calculated. Also, the surface tensions and viscosities of the treatment fluids were measured.

Lab results indicated that α-ZrP nanofluid mitigated fines migration in Berea sandstone up to 300°F. Because fresh water tends to cause formation damages, nanoparticles diluted with brine showed less permeability change than those diluted with

DI water. The best treatment we had was the α-ZrP nanofluid diluted with brine (5 wt% KCl) at a concentration of 0.5 wt%.

To use α-ZrP nanofluids as an EOR agent, Indiana limestone core was pre-flushed with brine, and then saturated with oil (dodecane). In addition, brine was injected again with different flow rates of 0.5, 1.0 and 2.0 cm^3/min for about 5 PV each. After that, 1 PV of EOR agent was injected at 0.5 cm^3/min from bottom to top. A post-flush of brine was applied and the effluents were collected to find out the total oil recovered. The test result gave a 13.68% oil recovery in the EOR stage.

The alpha-phased zirconium phosphate nanofluids had never been applied before for subsurface use. It was discussed as an clay stabilizer and EOR agent in this study. This work provides new insights into the application of nanoparticles in the oil and gas industry.

DEDICATION

To my husband and parents.

ACKNOWLEDGEMENTS

I would like to thank my committee chair, Dr. Hisham Nasr-El-Din, for his patients, guidance and encouragement through my master's work. In addition, I would like to thank my committee members, Dr. El-Halwagi and Dr. Jerome Schubert, for their guidance and support throughout the course of this research.

Thanks also to my friends and colleagues and the department faculty and staff for making my time at Texas A&M University a great experiences. Also, I would like to thank my family for their support.

NOMENCLATURE

P	Pressure, psi
t	Time, minutes
Q	Flow rate, cm^3/s
A	Cross-sectional area to flow, cm^2
k	Permeability, md
μ	Fluid viscosity, cP
γ	Shear rate, s^{-1}
K	Reaction constant
f	Activity coefficient

TABLE OF CONTENTS

Page

LIST OF FIGURES

Page

LIST OF TABLES

Page

1. INTRODUCTION

Nanoparticles often refer to particles with a very small sizes less than 100 nm. The nanofluids are created by the addition of nanoparticles to fluids for intensification and improvement of some properties at low volume concentrations of the dispersing medium (Suleimanov et al. 2011). Suspensions of nanodimensional particles can increase sedimentation stability, because its relative large surface forces easily counterbalance the force of gravity. They also have more stable thermal, optical, stress-strain, electrical, rheological and magnetic properties at high temperature and high pressure because of their smaller size. The evaluations of using alpha-zirconium phosphate nanofluid as a clay stabilizer and an EOR agent were performed in this study.

1.1 Usage of Nanoparticles as Clay Stabilizers

Fines migration is the movement of fine clay, quartz particles or similar materials within the reservoir formation due to drag forces during production. It reduces the productivity of well because the particles in produced fluid block the pore throats near the wellbore. Colloidal and hydrodynamic forces are found to be responsible for the fines detachment and their release from the pore surfaces. London Van der Waals attraction, double layer forces are the most dominant forces in the detachment of fines from porous media based on the DLVO theory (Habibi et al. 2012). In sandstone formations, when fresh water or high pH fluids are leaked-off or injected, fines migration becomes a big challenge.

To handle sand production from wells, both mechanical method and chemical method are used in the industry. The most common mechanical methods are applied by placing gravel packs, slotted-liners or sand screens downhole during well completion to prevent sands come into the well from formations. However, they are not the best option because they do not specifically address the cause of the problem, and results in loss of production time during cleaning and sometimes is ineffective (Ogolo 2013). Besides, these methods always come with the risks of formation damage and reducing of the production. For chemical methods to reduce fines migration, treatments such as resins, polymers, acids and several inorganic compounds are injected to stabilized the formations. The use of nanoparticles in control of fines migration has been found to be possible and is still under investigation (Ogolo 2013). This paper is aiming at finding an effective nano-treatment as clay stabilizer for sandstone formation.

A clay stabilizer is a chemical additive that is used to prevent migration or swelling of clay particles. Without adequate protection, water-based fluids can affect the electrical charges of naturally occurring clay platelets in the formation. Modifying the charge causes the platelets to swell or migrate in the flowing fluid. Clay stabilizers act to retain the clay platelets in position by controlling the charge and electrolytic characteristics of the treatment fluids (I.A. El-Monier et al. 2013).

Clay stabilizers can be divided into the following classes: simple inorganic salts, cationic inorganic polymers, cationic organic polymers, anionic organic polymers, and nonionic organic polymers (Zhou et al. 1995). Many researches are conducted. Ultra thin films of polymers have been reported to give good results (Sharma et al. 1994) as well as

water based agglomerating agents (Nguyen et al. 2010). Ross (1967, 1968) and Reed (1972) described the use of hydroxyl-aluminum as a treatment for fines migration. Screening studies were used to evaluate the performance of ionic liquids as KCl substitutes, clay stabilizer additives and shale inhibiters by Berry et al. (2008). A non-toxic, no smell, environmentally friendly Al/Zr based compounds was found to be effectively as clay stabilizer after using 15 wt% HCl acid washes by El-Monier and Nasr-El-Din (2013).

Newly, the search for applications of nanotechnology as a solution to reduce the formation damage caused by fines migration attracts the attention of many researchers. Nanoparticles are ideal for use in oil field applications due to their large surface area to mass ratio as well as their small size, chemical and thermal stability, and environmental friendliness (Belcher et al. 2010). Because of their very small size, nanoparticles can stay in the smallest pores without changing the total permeability and porosity of formation. Because of their very large surface area, they generate high surface forces and electrostatic forces between the treatments and formations to stabilize the loose particles.

Huang et al. (2008) introduced the use of nanoparticles for fines fixation in proppant packs. The results showed that nanoparticles stuck the fines firmly in place by changing the surface characteristics of porous media. Ahmadi et al. (2013) discussed the zeta potential of MgO, SiO_2 and Al_2O_3 nanoparticles deposited on rock surface to reduce fines migration. The total energy of interactions revealed that MgO has the highest tendency to use as clay stabilizer compared to the rest two treatments. Belcher et al. (2010) studied a field case in the Gulf of Mexico to indicate that the nanoparticles used have the

ability to remove and contain not only problematic clays, but also non-clay particles. The relationships between the pH values and the effectiveness of nano-treatments are evaluated by Ogolo et al. (2013). They found that a lower pH value gave a better result with a high zeta potential. Also, the presence of crude oil can alter the performance of nanoparticles in trapping fines in formations (Ogolo et al. 2013).

Electrostatic force of adsorption is the main reason for nanoparticles to stabilize fines in sand. Sandstone formations with anionic surface charges are attracted by nanoparticles with cationic surface charges. This attraction results to relatively strong bonds between the sand particles and the treatments. In this study, synthesis of α-ZrP based nanofluid was discussed. The effects of using this type of nanofluid as a clay stabilizer using Berea sandstone cores were experimentally tested to prevent fines migration.

1.2 Nanofluid Enhanced Oil Recovery

Enhanced oil recovery (EOR) is also known as improved oil recovery or tertiary recovery. An oil recovery enhancement method using sophisticated techniques that alter the original properties of oil. Once ranked as a third stage of oil recovery that was carried out after secondary recovery, the techniques employed during enhanced oil recovery can actually be initiated at any time during the productive life of an oil reservoir. Since the total rate of the oil production is nearing the decline phase in many place of the world, EOR had been researched and applied to fields for decades to extract more oil.

Waterflood is the most common method for secondary oil recovery. In waterflooding, water is injected into formation through injection wells in order to increase

the sweep efficiency and maintain the reservoir pressure above the bubble point. Waterflood worked well in many field cases; however, some oil was still trapped down in pores or pore throats with smaller sizes at macroscopic and microscopic scale.

The three major types of enhanced oil recovery operations are chemical flooding, miscible displacement, and thermal recovery. In most cases, chemical EOR includes the flooding of polymers, surfactants, alkali or any combination of the three. In general, the surfactant is responsible for reducing the interfacial tension between oil and water phases to a level that promotes the mobilization of trapped oil drops. The alkaline is intended to react with the acids to generate in-situ surfactant to overcome the surfactant depletion in the liquid phases due to retention. It also alters rock wettability and adjusts pH and salinity. The role of the polymer is to increase the viscosity, reducing the mobility ratio and hence allowing a greater volumetric swept efficiency. Fletcher et al. (2010) proposed six forces relevant in chemical EOR in **Table 1** and the complexity and scale-up for EOR processes were discussed.

Table 1 Six Forces Relevant in EOR (Fletcher et al. 2010)

Force	Nature of Force
Coulombic	The intermolecular forces. There comprise van der Waals forces: induced dipole (London), dipole-dipole and hydrogen bonding forces. If polar molecules and ions are present then ion-dipole and ionic bonding forces exist.
Disjoining	Forces associated with thin films due to the departure from bulk properties arising from the influence of the surfaces. Includes steric and double layer forces – as well as van der Waals forces
Marangoni	Forces that arise due to a gradient in a property such as concentration or interfacial tension. An example of Marangoni forces is 'tears of wine' – the roll up of wine into droplets when swirled around a clean glass
Capillary	Forces resulting from the curvature of fluid interfaces which yields pressure differences between the different fluid phases
Viscous	Forces associated with the viscosity contrast of fluids and responsible for the displacement efficiency of one fluid by another
Gravity	Forces responsible for water/oil separation on the macroscopic scale due to density differences, and hence buoyancy effects.

Many researchers had investigated the oil recovery mechanism using nanoparticles suspension. Ayatollahi et al. (2012) believed that electrical double layer generated between the particles and the formation is the main reason according to the DLVO theory. DLVO theory explains the aggregation of aqueous dispersions quantitatively and describes the force between charged surfaces interacting through a liquid medium.

It can also be used to simulate the interactions of nanoparticles with each other (Aggregation), to other particles present in the medium and also with rock surface

(Adsorption) for wettability changes (Ayatollahi et al. 2012). Das et al. (2008) and Wasan et al. (2011) described the mechanism as the disjoining pressure mechanism in **Figure 1**. They found that a wedge-film structure was generated and the structural disjoining pressure lead to a decrease of the contact angle of the nanofluid to 1°. Hendraningrat et al. (2013) studied the two-phase flow nanofluid EOR using transparent glass micromodel. The residual oil saturation was reduced shown in **Figure 2**.

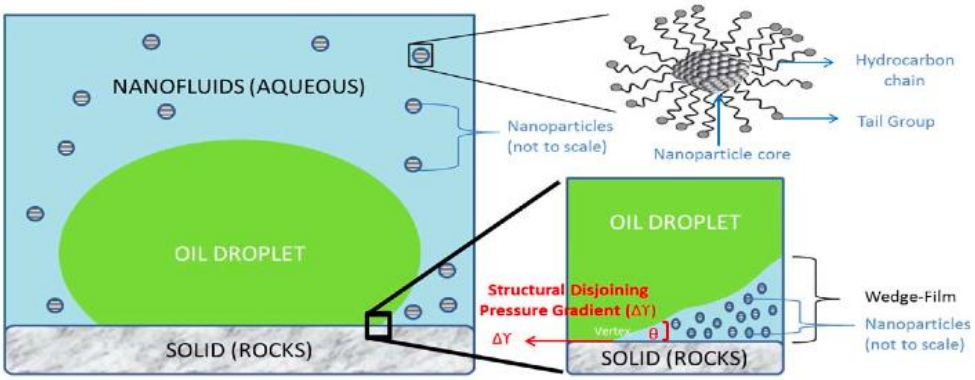

Figure 1. Illustration of nanoparticle schematic and structural disjoining pressure gradient mechanism among solid, oil and nanofluids as aqueous phase due to nanoparticles structuring in the wedge-film (Hendraningrat et al. 2013)

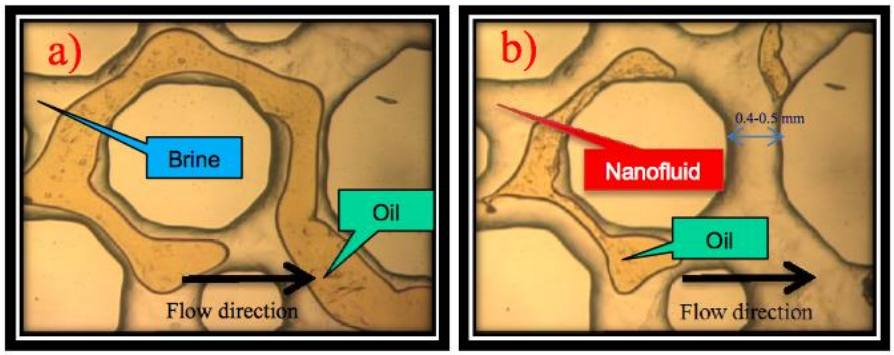

Figure 2. Residual oil inside pore network of glass micromodel under microscope (Hendraningrat et al. 2013)

According to Kong (2010), nanoparticles offer a way to control oil recovery processes that is unmatched by any current or previous technology. Because they can improve the geomechanics of a reservoir, and can tune up the viscosity of the injected fluid, such as CO_2 or surfactant, to an optimum level. In addition, the emulsification of nanoparticles could be used as oil recovery agent because of its stability. Also, the emulsification could form a compact layer of nanoparticles at the droplets interface.

The effectiveness of using nanoparticles as EOR agent was still under debate. Suleimanove et al. (2011) used nanoparticles to get an increased 1.5 fold oil recovery in comparison with the aqueous solution of anionic surface-acting agent and 4.7 fold in comparison with water. They also found that nanoparticles decreased surface tension 70 – 79%. However, Hendraningrat et al. (2013) thought although nanofluid were able to decrease IFT and alter wettability, additional recovery was not guaranteed in low-medium permeability water-wet Berea sandstone. Their results also performed that higher

concentration had a tendency to block pre network and would not give additional oil recovery in low permeability reservoir.

In this study, an emulsion of alpha-ZrP nanoparticles was used as an EOR agent. Coreflood test was conducted and the mechanism and results will be discussed.

2. SURFACE TENSION AND VISCOSITY

2.1 Materials and Equipment

Alpha-ZrP based nanofluid as a clay stabilizer was obtained in aqueous solution with both DI water and 5 wt% KCl. The α phase of zirconium phosphate with the chemical formula $Zr(HPO_4)_2.H_2O$ (**Figure 3**) is one of the most widely used lamellar crystals.

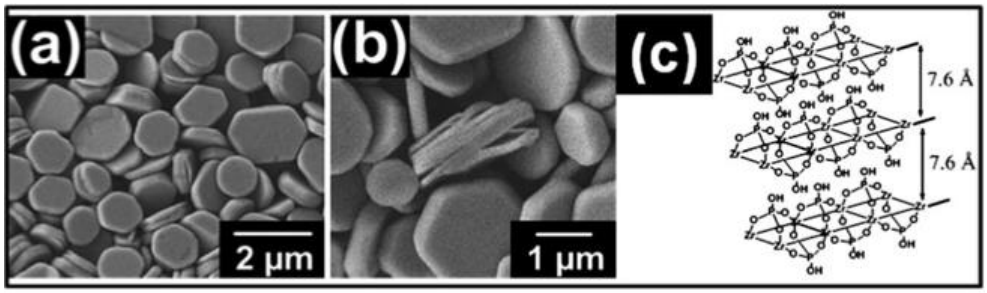

Figure 3. The alpha-zirconium phosphate crystals (Mejia et al. 2012)

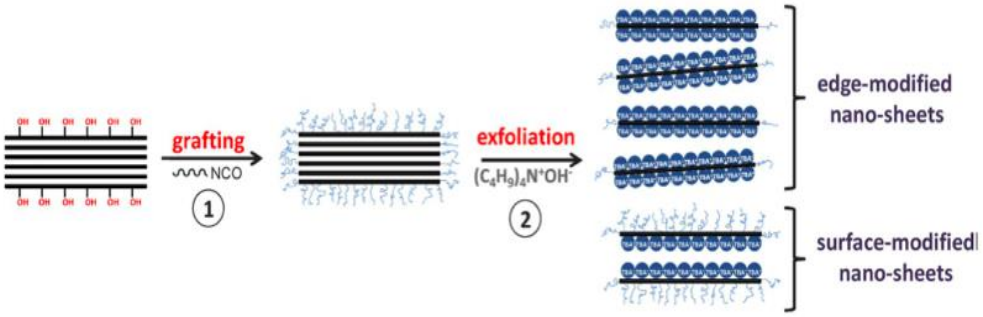

Figure 4. The 2-D schematic representation of the fabrication of surface and edge-modified amphiphilic nano-sheets.

1The α-ZrP crystal layer is composed of a ZrO_6 sheet coordinated with HPO_4^{2-} tetrahedrons forming a covalent network. The thickness of a monolayer of α-ZrP is about 0.66nm (Mejia et al. 2012). Since α-ZrP is strongly hydrophilic, chemical modification is applied to make it hydrophobic. First, a coupling is grafted over the exposed edges and flat surfaces of the α-ZrP crystals. Then, via the exfoliation of these crystals, a mixture of surface and edge-modified amphiphilic nano-sheets are obtained from the outer and inner layers (**Figure 4**). The resulting nano-sheets are amphiphilic (Mejia et al. 2012). The surface tensions and viscosities of both α-ZrP modified with TBA^+ (tetra-(n-butylammonium)) and glucose were tested. The reaction mechanism for modification agents grafting over the edge and the outer surfaces of alpha-ZrP crystals was given in **Figure 5**.

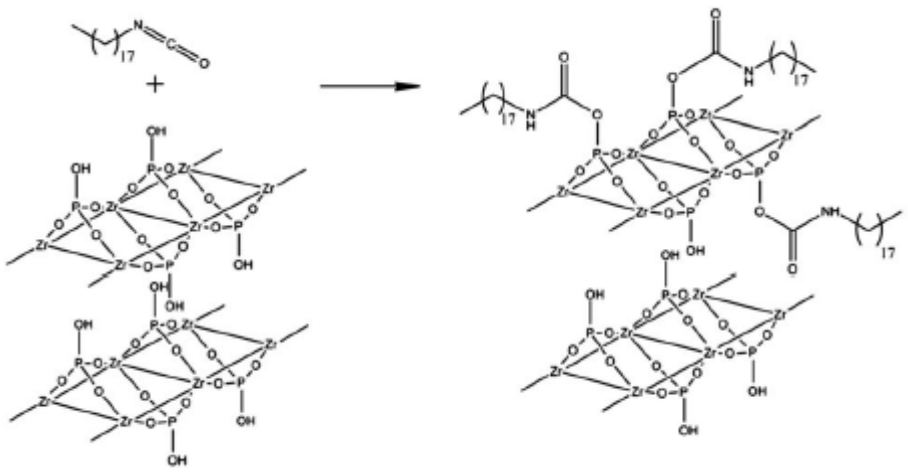

Figure 5. Reaction mechanism for modification agents grafting over the edge and the outer surfaces of alpha-ZrP crystals

Surface tensions were measured with EasyDyne tensiometer (**Figure 6**) at room temperature. Viscosity measurements were conducted using a HT/HP viscometer **(Figure 7**) at both 78°F and 245°F.

Figure 6. EasyDyne Tensiometer

Figure 7. High Temperature/High Pressure Rheometer

2.2 Experimental Procedure

The surface tension of both α-ZrP modified with TBA^+ (tetra-(n-butylammonium) and glucose were tested at room temperature and atmosphere pressure. The platinum plate method was used. First, cleaned the plate with distill water and dry it with flame till red. Then suspended the cleaned plated from the hook at the force sensor. Filled the distill water about one third to half of the vessel SV 20. After that, selected the 'Wilhelmy Plate" method. The surface tensions of both fluids were measured at concentrations of 0.01, 0.025, 0.075 and 0.1 wt%.

Apparent viscosities of the fluids were measured at different shear rates. The measurements were conducted in the order of ascending shear rates from 0.1 to 1,000 s^{-1} at room temperature. Then, the shear rate was fixed at 100 s^{-1} by increasing the test

temperature from 75 to 245°F. When measuring the storage modulus G' and the viscous modulus G", the first series of tests were conducted by increasing the frequency from 0.3 to 5 Hz. Then, the moduli were measured at 1 Hz by increasing the temperature from 75 to 220°F. A pressure of 300 psi was applied during high temperature measurements. The viscosities of both α-ZrP modified with TBA (tetra-(n-butylammonium) and glucose were tested.

2.3 Results and Discussion

2.3.1 Surface Tension Measurements

The results of surface tension measurements at room temperature and atmosphere pressure of α-ZrP-TBA and α-ZrP-glucose were given in **Table 2** and **Table 3**.

Table 2 Surface Tension of α-ZrP-TBA

	Concentration (wt%)					
Trial	0.01	0.025	0.05	0.075	0.1	0.01
1	61.3	59.2	60.2	55.2	57.9	57.1
2	63.6	60.9	61.3	57.6	58.5	57.5
3	63.7	61.3	61.3	58.3	58.6	57.8
4	63.7	61.4	61.5	58.3	58.8	58.2
5	63.6	61.4	61.6	58.2	59	58.3
Average	63.18	60.84	61.18	57.52	58.56	57.78

Table 3 Surface Tension of α-ZrP-glucose

	Concentration (wt %)				
	0.01	0.025	0.05	0.075	0.1
1	45.4	43.2	39	40.2	32.4
2	42.6	42.7	36.6	39.4	32.1
3	42.9	42.8	35.4	36.8	32.2
4	41.8	42.4	34.9	35.6	32.1
5	42.6	41.1	34.9	35.4	31.8
ge	43.06	42.44	36.16	37.48	32.12

For α-ZrP-TBA, **Figure 8** showed that as the concentration of the fluid gradually increased from 0.2 wt% to 1.3 wt%, the surface tension tended to decrease. The differences of the surface tensions are not significant. Also, the surface tensions of α-ZrP-TBA were only slightly lower than the surface tension of DI water. According to the value of its surface tensions, α-ZrP-TBA is not an ideal chemical treatment for enhanced oil recovery.

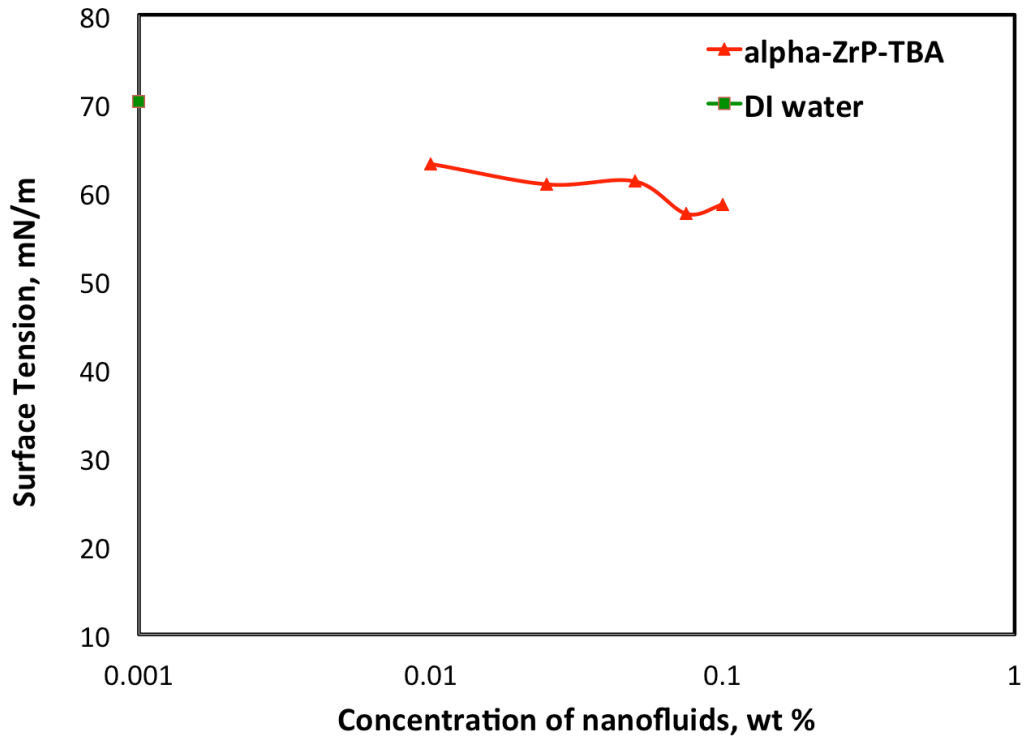

Figure 8. The surface tensions of α-ZrP-TBA versus the concentration of the fluid

For C18-ZrP-glucose, **Figure 9** showed that the surface tensions decreased from 43.06 to 32.12 mN/m as the concentration increased from 0.01 wt% to 0.1 wt%. The values

of the surface tensions of the treatment were less than half of the surface tension of DI water. If a higher concentration was applied, this treatment could work as an EOR agent.

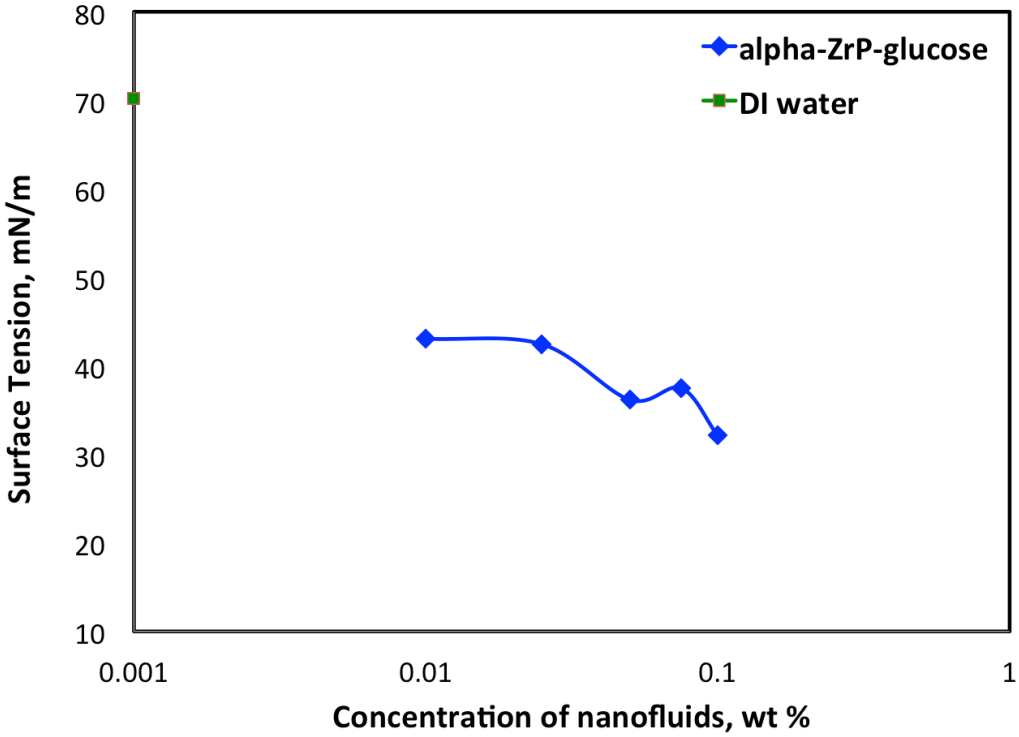

Figure 9. The surface tensions of α-ZrP-glucose versus the concentration of the fluid

2.3.2 Viscosity Measurements

The viscosities of α-ZrP-TBA and α-ZrP-glucose were given in **Figure 10** and **Figure 11**. With increasing of shear rate, obvious decreasing of viscosity was observed at both 25°C and 90°C. Although the viscosity of α-ZrP-TBA was higher than the viscosity

of α-ZrP-glucose at the beginning of the measurements, neither of them was considered as a real viscid fluid that could lead to formation damages. Both of the two fluids have shear thinning performances. According to the results of the viscosity measurements, both α-ZrP-TBA and α-ZrP-glucose would not cause formation damages because of their viscosities if used as subsurface treatments.

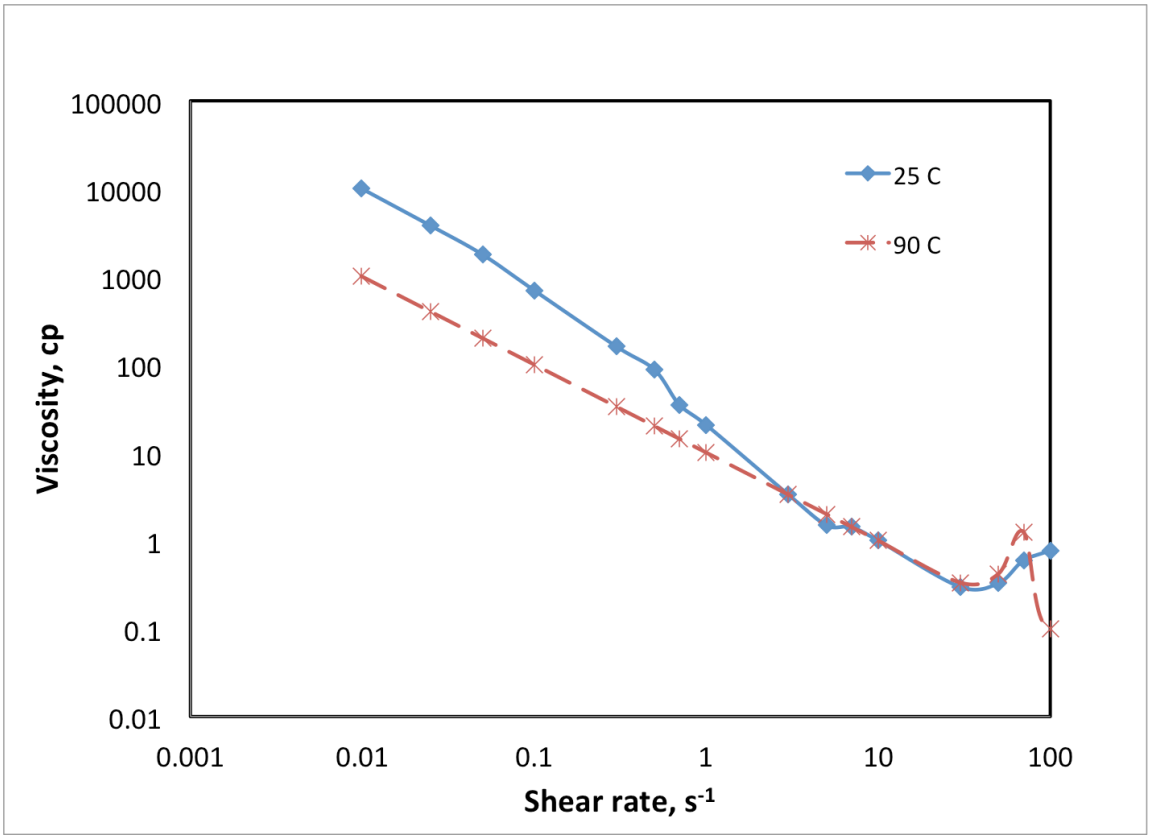

Figure 10. Viscosity of α-ZrP-TBA

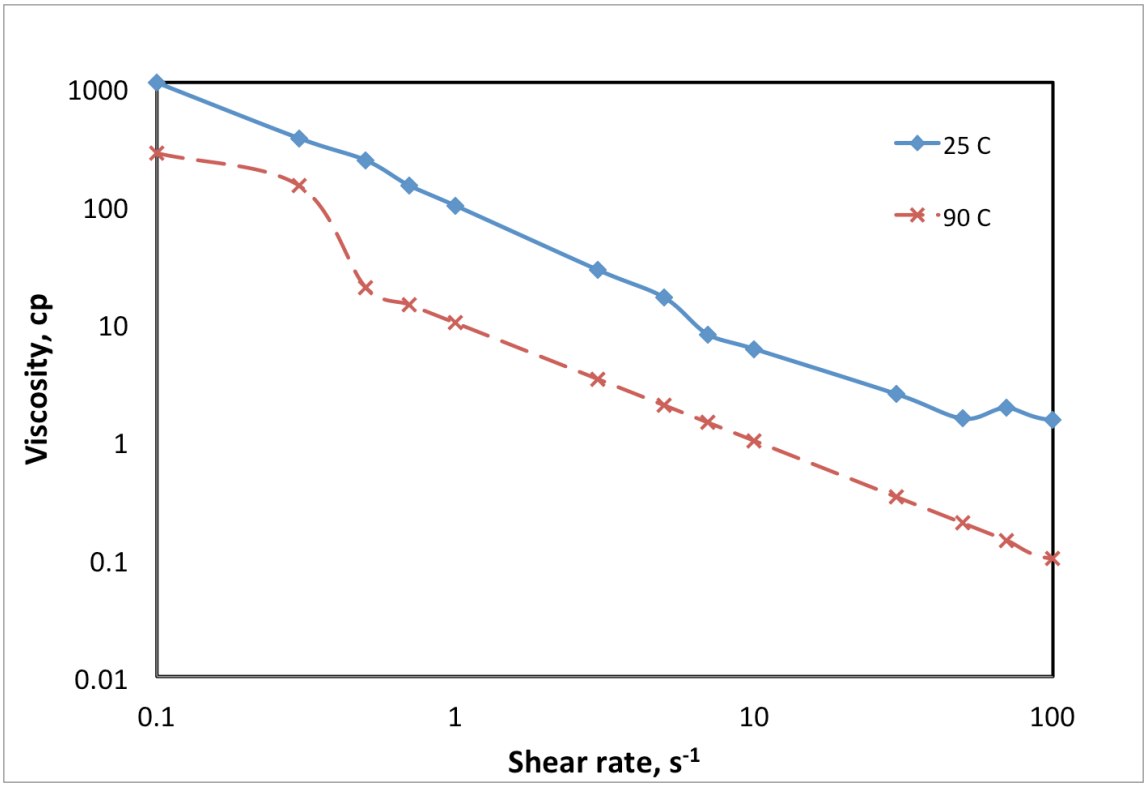

Figure 11. Viscosity of α-ZrP-glucose

2.4 Conclusion

According to the surface tensions measured at different concentrations, α-ZrP-glucose might act better than α-ZrP-TBA as an EOR agent. Both of the two fluids were not viscid enough to create formation damages.

3. EVALUATION OF ALPHA-ZRP NANOPARTICLES AS A CLAY STABILIZER

3.1 Materials and Equipment

Different concentrations of α-ZrP-glucose were used in this experiment. As discussed before, α-ZrP-glucose nanofluids has cationic surface charge and a relative low surface tension. Since low salinity brine is always introduced into the formation by natural or artificial water flooding and enhances oil recovery, it is the most common fluid to initiate fine migration. The brine used in this experiment was prepared using 5 wt% KCl. Type of cores used in the coreflood tests was Berea sandstone. The cores were cut into a length of 6 inches and 1.5 inches in diameter.

The coreflood setup (**Figure 12**) was constructed to determine the permeability change before and after the injection of treatments into the core.

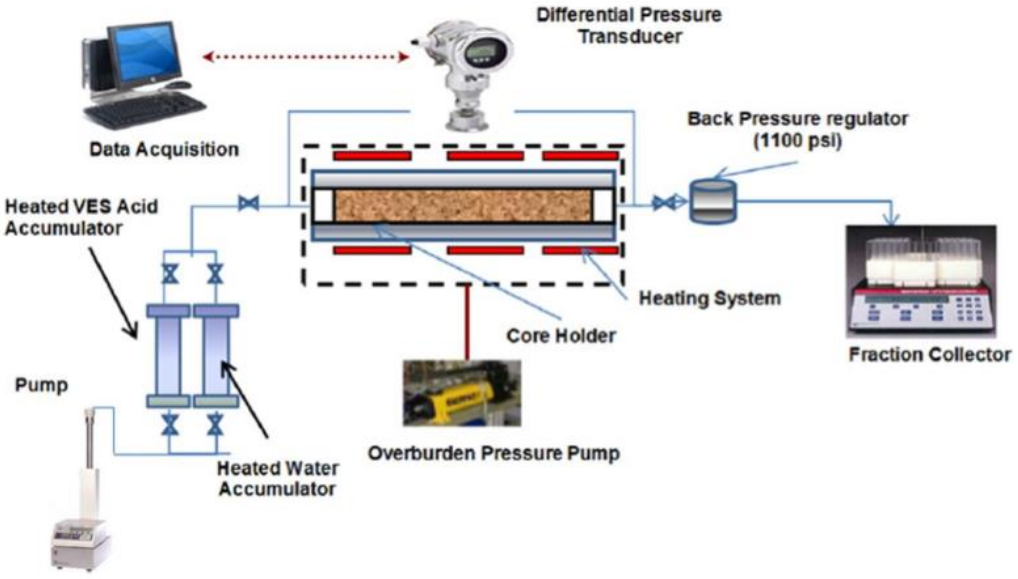

Figure 12. Coreflood setup.

Three transfer vertical vessels were connected to the core holder. From left to right, the first vessel can hold up to 2 liters of brine, the second vessel can hold up to 2 liters of DI water, and the third vessel can hold up to 1 liter of stabilizer. All three fluids were injected using a hydraulic pump. A nitrogen cylinder was used to apply backpressure, and an enerpac pump applied overburden pressure around the core. Pressure transducers were connected to a computer to monitor and record the pressure drop across the core during the experiments. Based on the maximum pump pressure and the backpressure, the maximum pressure drop across the core was 900 psi. An automatic fraction collector was used to collect the effluent fluids.

3.2 Experimental Procedure

While preparing the cores for coreflood tests, the cylindrical cores were dried at 250°F overnight to get the dry weight. Then, the cores were immersed in brine (5 wt% KCl) for 24 hours to insure full saturation to obtain the saturated weight. Porosities of the cores were calculated based on the two weight differences and the density of the brine.

Four coreflood tests were conducted. For all four tests, 5 wt% KCl solution was first injected at room temperature to the cores at a flow rate of 2 cc/min to get a relationship between the pressure drop and flow rate, so that the permeability of the cores could be calculated through Darcy's Law. Then, keep injecting 5 wt% KCl at 300°F till the pressure drop is stable. The stabilizer was injected for 1 pore volume after the pressure drop is not increasing. At last, DI water was flushed after the injection of treatments till pressure drop is stable again, to evaluate the effectiveness of the clay stabilizer by analyzing the permeability change. For Test 1, the nanoparticles suspension was diluted with DI water. For the rest three tests, the nanofluids were diluted with brine (5 wt% KCl). The procedure was given in **Figure 13**. The concentrations and the dilution agents of the treatments used for testing are given in **Table 4**.

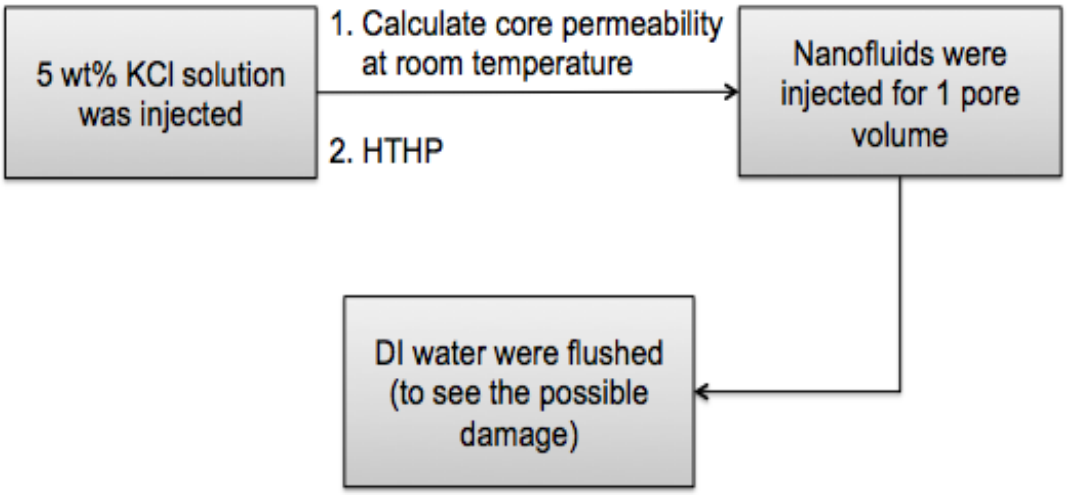

Figure 13. Coreflood Procedures

Table 4 The Concentrations and Diluting Agents of Nanofluid for Four Tests

	Nanofluid Concentration (wt%)	Diluting Agent
Test 1	0.1	DI water
Test 2	0.1	5 wt% KCl
Test 3	0.5	5 wt% KCl
Test 4	1.0	5 wt% KCl

Table 5 Properties of the Cores

	Permeability (md)	Pore Volume (cm^3)	Porosity (%)
Core 1	112.8	30.9	17.8
Core 2	100.0	34.0	19.3
Core 3	89.3	32.5	18.7
Core 4	71.4	32.3	18.6

Table 6 Mineralogy of Berea sandstone

Mineral	Concentration (wt%)
Quartz	86
Kaolinite	5
Feldspar	3
Chlorite	2
Calcite	2
Dolomite	1
Ilite	1

3.3 Results and Discussion

The permeability, pore volumes and porosities of the four cores in coreflood tests were listed in **Table 5**. The pore volume of the four cores ranged from 30.9 to 34 cm^3. The permeabilities of the cores ranged from 71.4 to 112.8 md. Darcy's Law was used to calculate the permeabilities.

$$Q = \frac{kA}{\mu L}\Delta p$$

The mineralogy of Berea sandstone cores was given in **Table 6**.

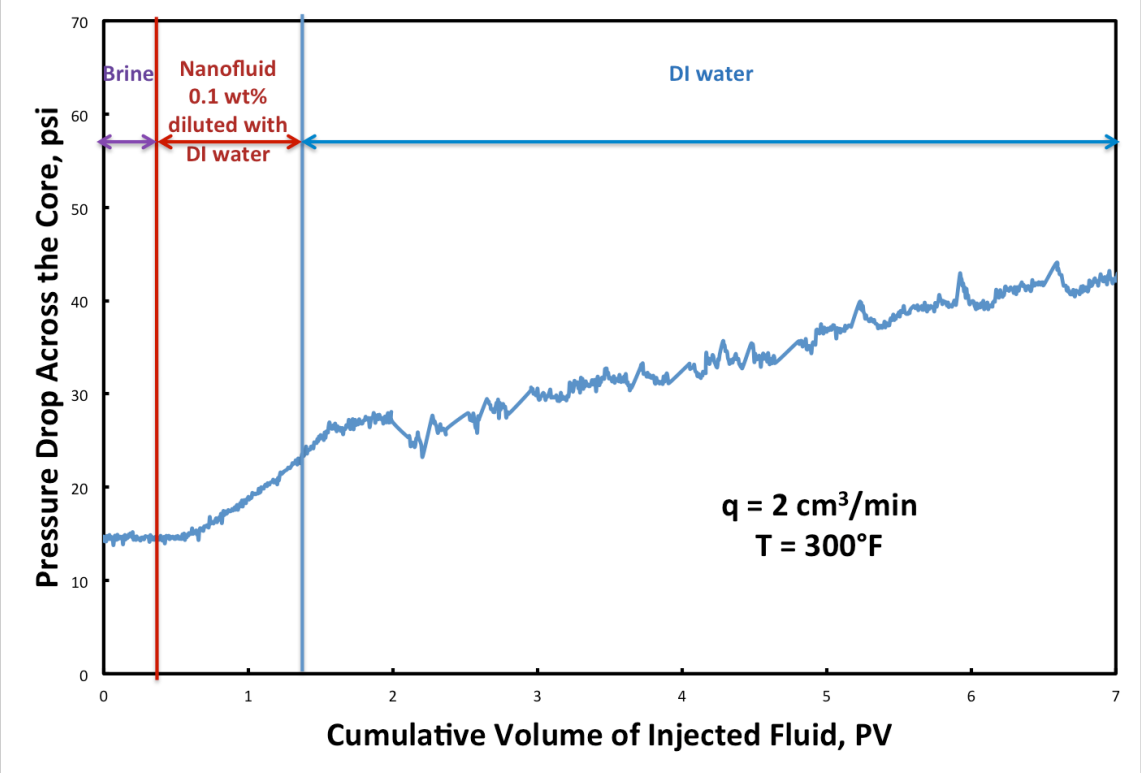

Figure 14. Coreflood performance of 0.1 wt% alpha-ZrP nanofluid diluted in DI water as a clay stabilizer.

In test 1, clay stabilizer was diluted with DI water to 0.1 wt%.

Figure 14 showed that pressure drop started to increase during the injection of the treatment, and kept increasing throughout the entire test. In the end, the pressure drop across the core increased from 14 psi to 42 psi. This treatment was not successful, because the increasing of the pressure drop during the whole process of the tests meant that the damage in the core was not prevented effectively. Fines were still kept blocking the pore throats, even at the time the treatment was injecting.

In test 2, the diluting agent of the treatment changed from DI water to brine (5 wt% KCl) to prevent the damage form the treatment fluid. The concentration of the clay stabilizer stayed the same at 0.1 wt%. **Figure 15** showed that the pressure drop remained constant while the treatment was injecting. It meant that the switching of the diluting agent prevent the damage of the core at this level. As the DI water was injecting after the treatment to try to create more damage, the pressure drop started to increase. This treatment solve the core damage at the time of injecting clay stabilizer, but still not effective at preventing further damage (**Figure 16**).

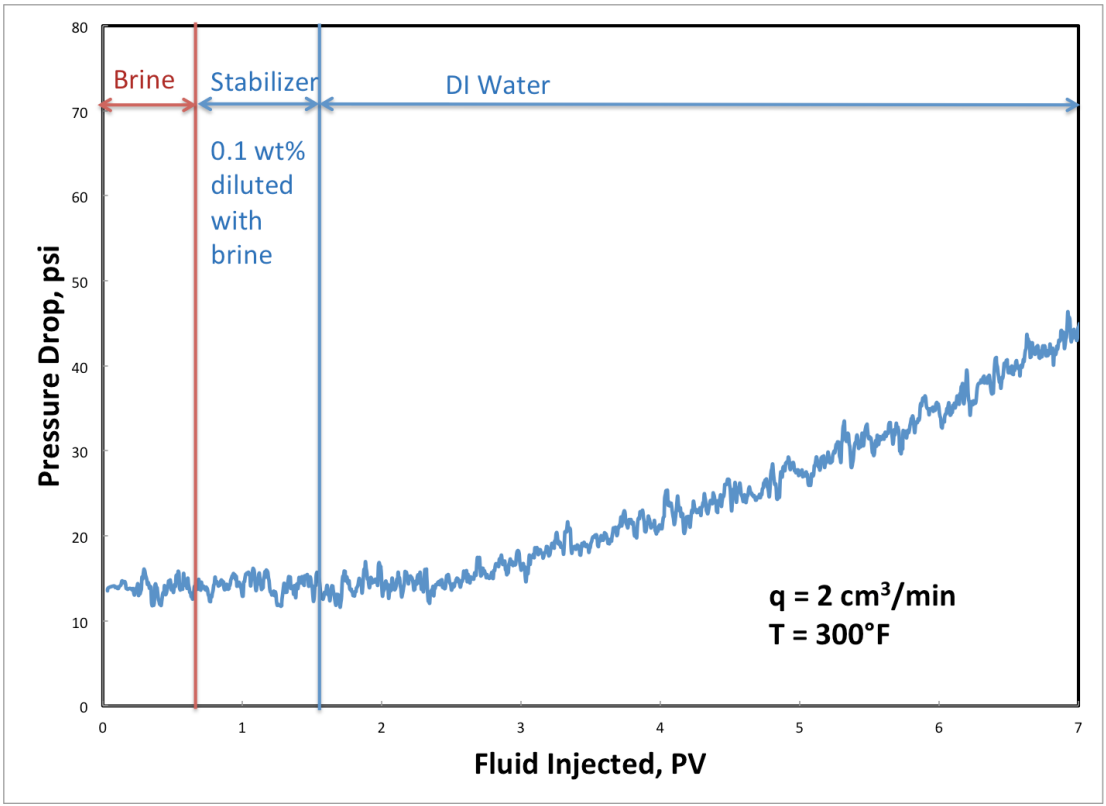

Figure 15. Coreflood performance of 0.1 wt% alpha-ZrP nanofluid diluted in brine as a clay stabilizer.

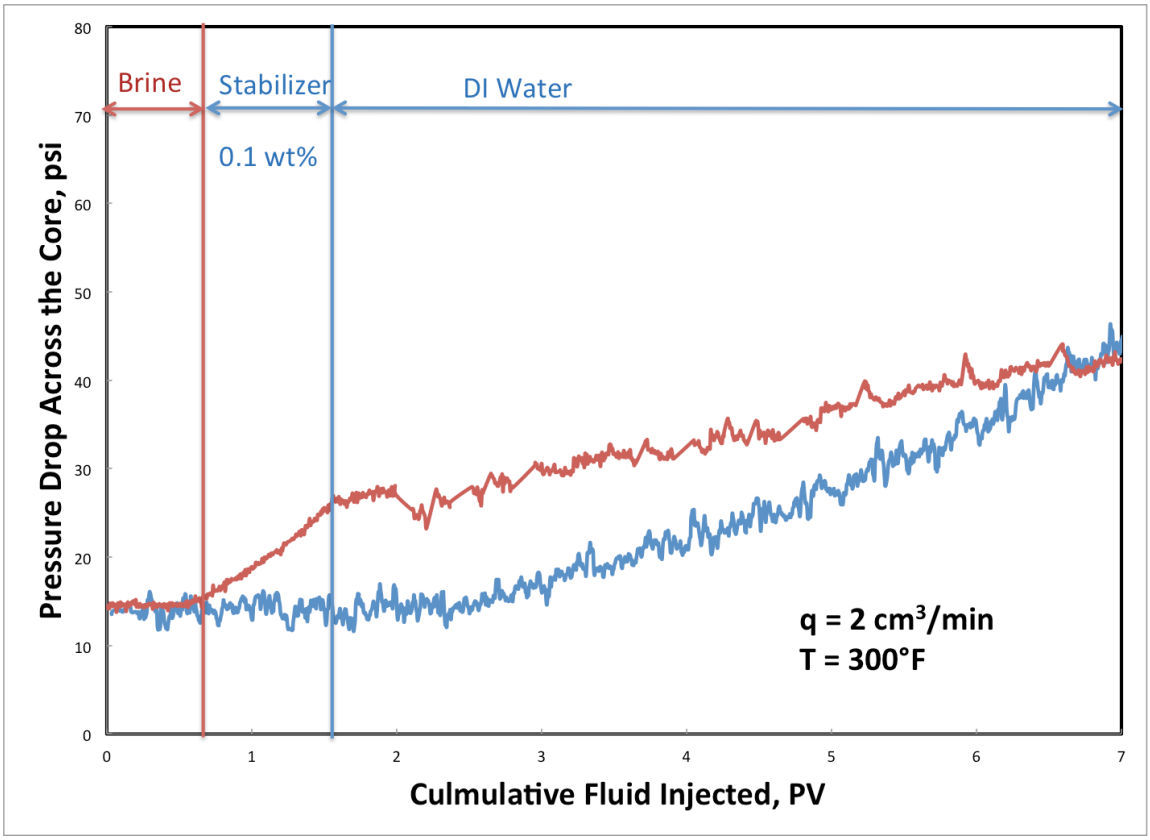

Figure 16. Comparison of using DI water and brine as diluting agent.

In test 3, a higher concentration of the treatment was applied. 0.5 wt% of α-ZrP-glucose nanofluid diluted with brine was injected at 2 cm^3/min. From Error! Reference source not found., no obvious increasing of pressure drop was observed at the first two stage of the treatment. It means that the permeability was controlled well at the flushing of both brine and clay stabilizer. In the post-flush, the pressure drop increased less than 10 psi after 7 PV of the DI water injection. This treatment prevented the damage during both the injection of the treatment and the injection of DI water.

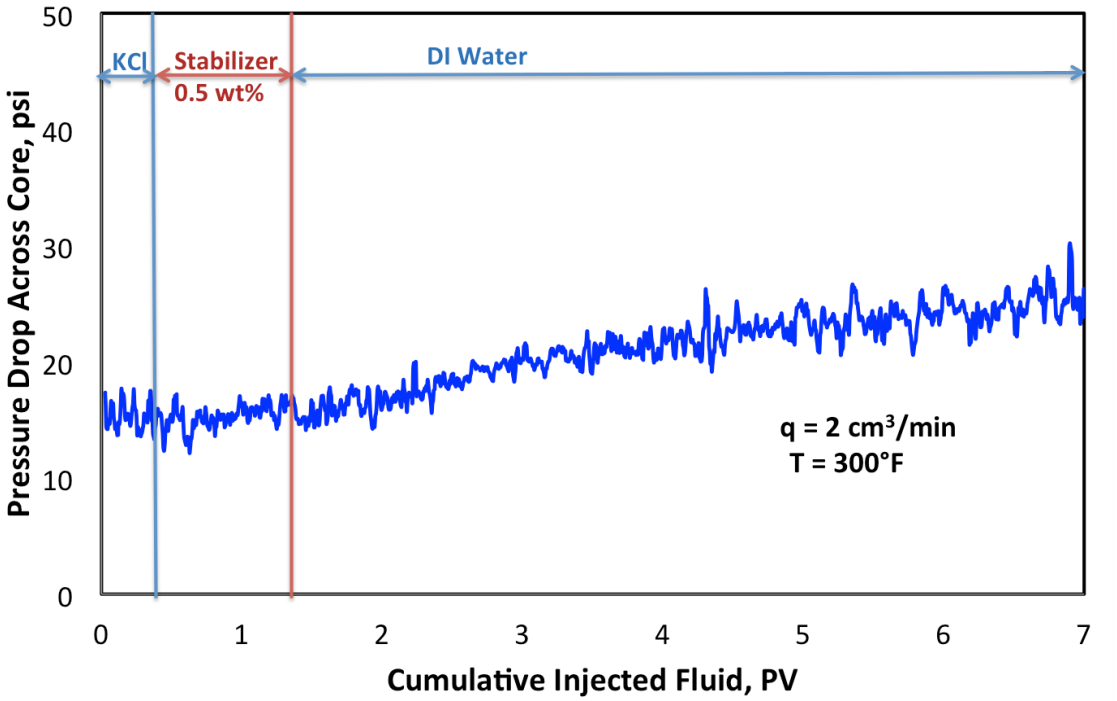

Figure 17. Coreflood performance of 0.5 wt% alpha-ZrP nanofluid diluted in brine as a clay stabilizer.

Since test 3 performed better than test 2, the concentration of the treatment was proved to be relative to the effectiveness of the clay stabilizer. Nanofluid at a concentration of 1.0 wt% was injected at test 4 to see if a better result can be generated. To prevent the damage at the stage of nanofluid injection, brine was still used as the diluting agent.

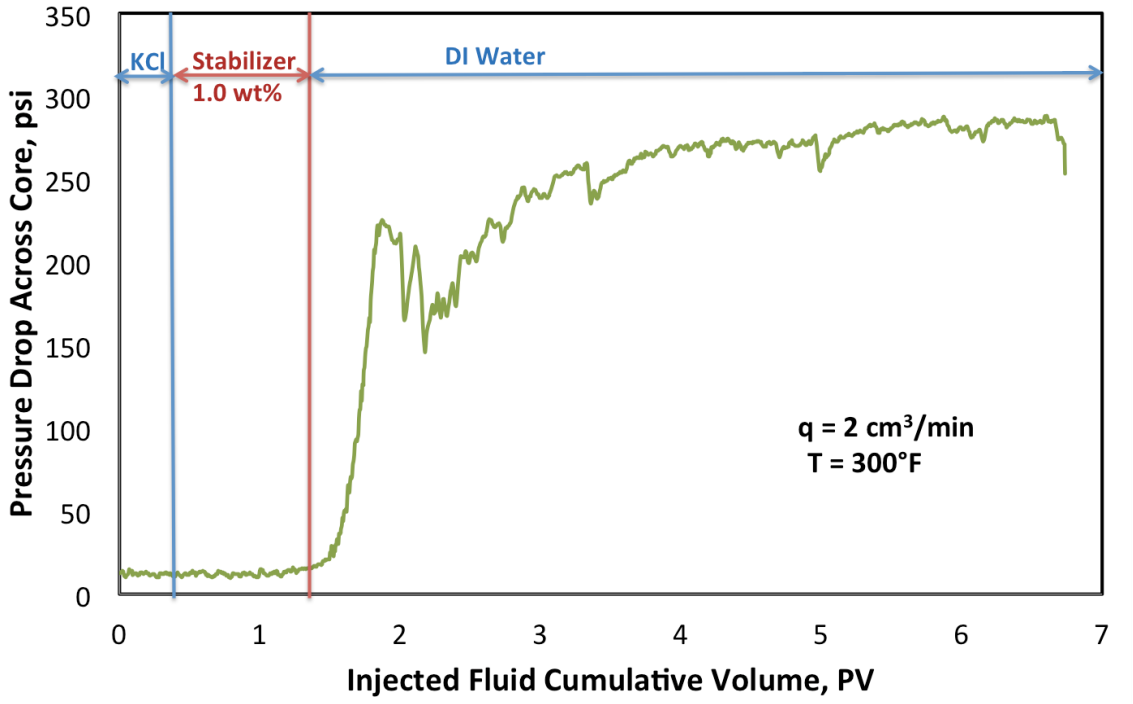

Figure 18. Coreflood performance of 1.0 wt% alpha-ZrP nanofluid as a clay stabilizer.

Figure 19. White residues at the inlet of the core.

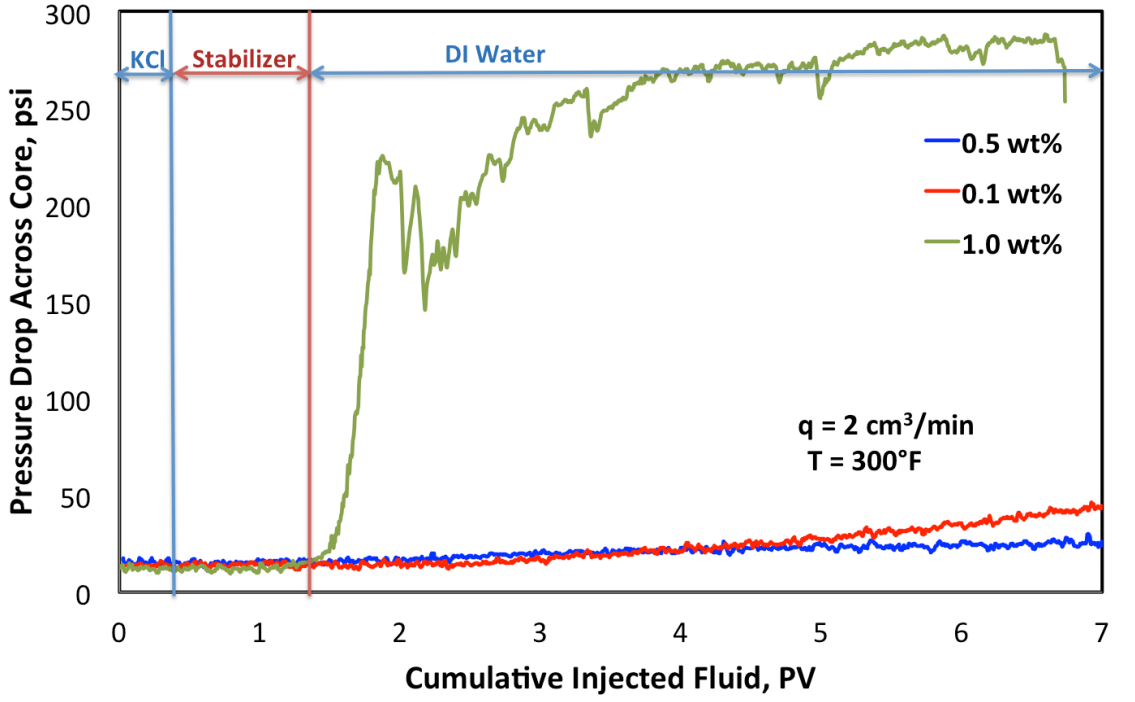

Figure 20. Comparison of pressure drop across the core of test 2, test 3 and test 4.

Figure 18 gave the results of test 4. From the figure, a huge increasing of pressure drop was observed at the beginning of the DI water injection. Within the first pore volume injection of DI water, the pressure drop increased from 10 psi to 220 psi, then kept increasing till 280 psi at the time when 7 pore volume of total fluid was injected. This indicated that the core was damaged dramatically at start of the injection of DI water. The reason of this sharp decreasing of the permeability was found out when the core was taken out from the core holder. **Figure 19** is the photo taken of the inlet of the core after the treatment. The white solids residue observed in the inlet of the core was the suspension of the nanofluid. The nanoparticles were not dissolved in DI water and brine, but existed as

suspension in the fluid. When the concentration of the treatment was too high, such as 1.0 wt% in test 4, the suspended particles could not enter the pore space and resided at the inlet as solids to cause the damage of the core. A comparison of pressure drop across the core of test 2, test 3 and test 4 was shown in **Figure 20**.

3.4 Conclusion

Alpha-ZrP-glucose worked effectively as a clay stabilizer testing with Berea sandstone at high temperature and high pressure. The concentration played a role in the effectiveness of the treatment. A higher concentration may lead to a better result, however, if the concentration was too high (1.0 wt%), the pore throat would be blocked and more damages would occur. Treatment of 0.5 wt% diluted in 5 wt% of KCl gave the optimal result. It prevented the core damage during the injection of both nanofluid and DI water, and would not cause any further damage.

4. ALPHA-ZRP NANOPARTICLES IN ENHANCED OIL RECOVERY

4.1 Introduction

Pickering emulsions are emulsions stabilized by colloidal particles. Water-in-oil Pickering emulsions are the reason for the high stability of water droplets in crude oil (Mejia et. al 2012). The emulsion is formed when solid particles are adsorbed on the water-oil interface, so that the surface energy of the system is reduced. Nanoparticles are much smaller than colloidal particles in sizes, and the emulsions stabilized by nanoparticles can travel a longer distance in reservoirs without much retention (Zhang et al. 2010). Also, specific characteristics can be made to nanoparticle emulsions, so that the formation and rheological properties of the emulsions can be well controlled.

Zhang et al. (2010) studied the phase behavior of both decane-in-water and water-in-decane emulsions with hydrophilic and hydrophobic nanoparticles. They gave the contact angle on particle surface and its relation with emulsion structure in **Figure 21**. In addition, they found that the emulsion rheology is strongly shear-thinning for both emulsions, and those characteristics have potential to facilitate the conformance control during oil recovery.

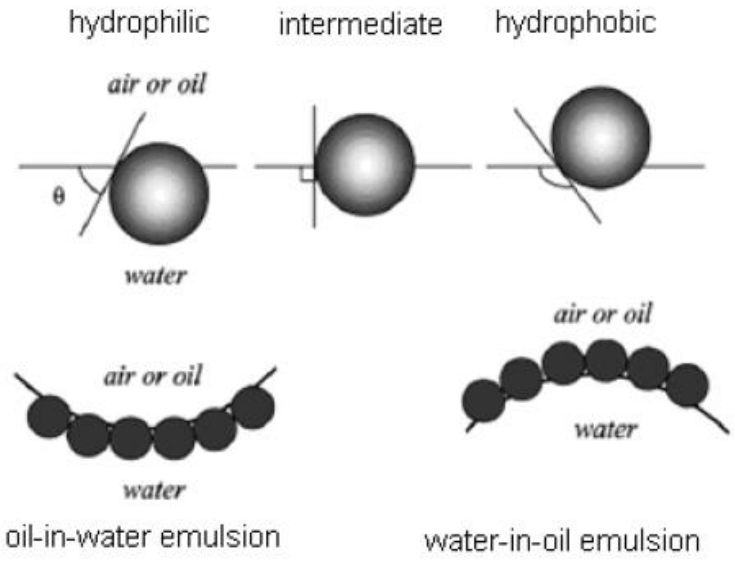

Figure 21. Contact angle on particle surface and its relation with emulsion structure.

4.2 Materials and Equipment

An alpha-ZrP nanoparticles in water emulsion (**Figure 22**) was used as EOR agent. The interfacial tension between water and the emulsion was 10^{-4}N/m. The particle size of the emulsion was around 200 nm. In zeta potential tests, diluted aqueous suspension of ZrP platelets (without glucose) was tested by using Zetasizer Nano ZS90 (Malvern Instruments Ltd, UK). The equipment was shown in **Figure 23**.

In coreflood tests, dodecane was used as the crude oil. Indiana limestone has well connected intergranular pores with medium to large sizes. The pore throat diameter was larger than 16 μm. High permeability Indiana limestone core was cut into a diameter of 1.5 in and a length of 6 in. The coreflood setup was similar to the setup described in **Figure 12**. Instead of DI water, dodecane was injected from the accumulator.

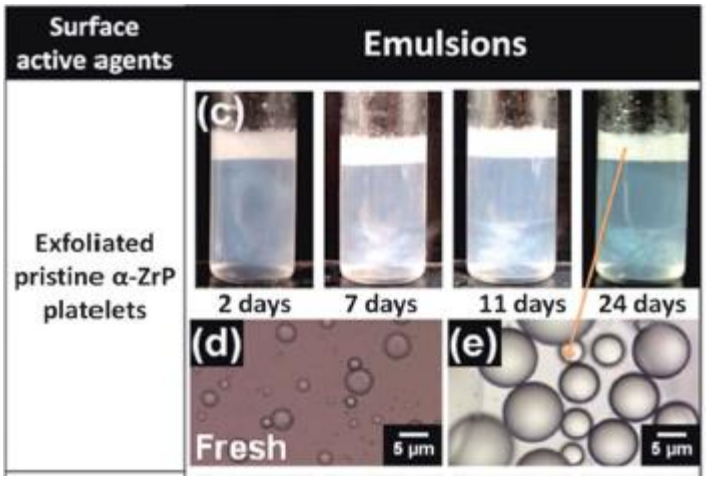

Figure 22. Emulsions of exfoliated pristine alpha-ZrP used (Mejia et al. 2012)

Figure 23. Zetasizer Nano ZS90 (Malvern Instruments Ltd, UK)

4.3 Experimental Procedure

4.3.1 Zeta Potential Measurements

Zeta potential is the potential difference between the dispersion medium and the stationary layer of fluid attached to the dispersed particle. *The zeta potentials of 0.5 wt%* diluted aqueous *suspension of ZrP without glucose were* measured at 76.7, 94.7, 112.7 and 130.7°F.

4.3.2 Coreflood Tests

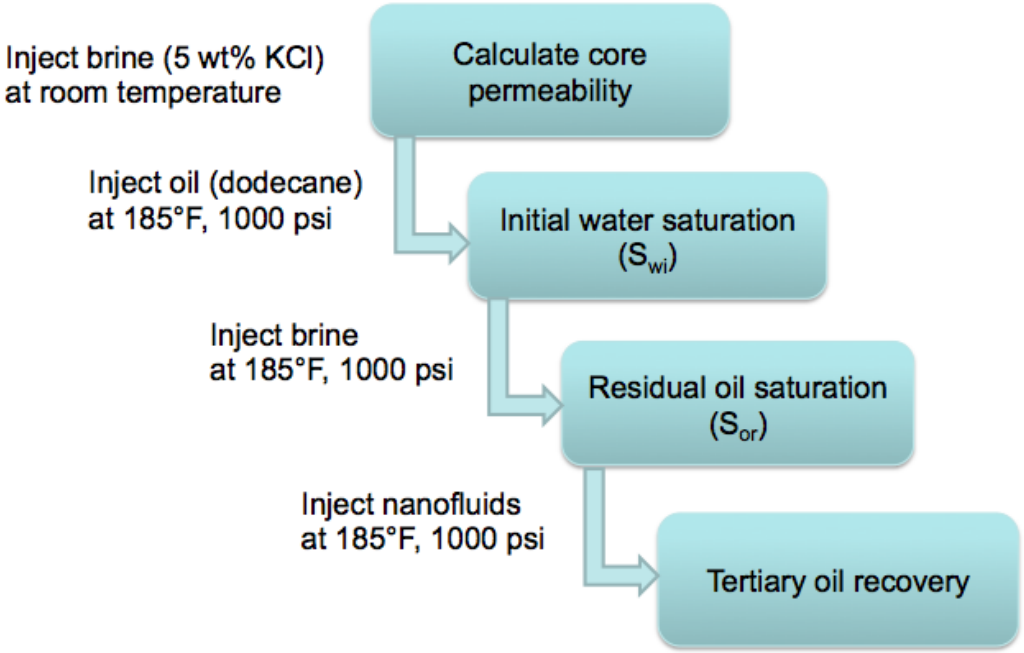

Figure 24. Coreflood Procedure for EOR experiment.

The procedure of the coreflood test was given in **Figure 24**. At first, the Indiana limestone core was dried in the oven at 250°F for 6 hours. Then, it was fully saturated

with brine (5 wt% KCl) using a vacuum pump four 4 hours. From the dry weight and the saturated weight of the core, the porosity and the pore volume of the core were calculated known the density of the brine. After put the core into the core holder, brine was injected from the top of the core to create a larger area of the fluid channel inside the core. By measuring the pressure drop across the core at different flow rates, the permeability of the core was calculated based on Darcy's Law.

To create initial oil saturation, dodecane was injected at flow rates of 0.1, 0.2, 0.4, 0.6, 0.8, 1.0, 1.5, 2.0, 3.0 and 4.0 cm^3/min till reach stabilization. With the total fluid and the total brine collected after the oil injection, the initial water and oil saturation were calculated. The secondary recovery was conducted by injecting brine into the oil saturated core. The brine was injected with different flow rates of 0.5, 1.0 and 2.0 cm^3/min for about 5 PV each. After that, 1 PV of EOR agent was injected at 0.5 cm^3/min from bottom to top. A post-flush of brine was injected at 0.5 and 1.0 cm^3/min for 5 PV each to make sure to get the maximum amount of oil. Effluents were collected after each level of recovery to get the amount of recovered oil. A backpressure of 300 psi and an overburden pressure of 750 psi were applied. The flow chart in Figure 25 gave the procedure of the tertiary oil recovery process.

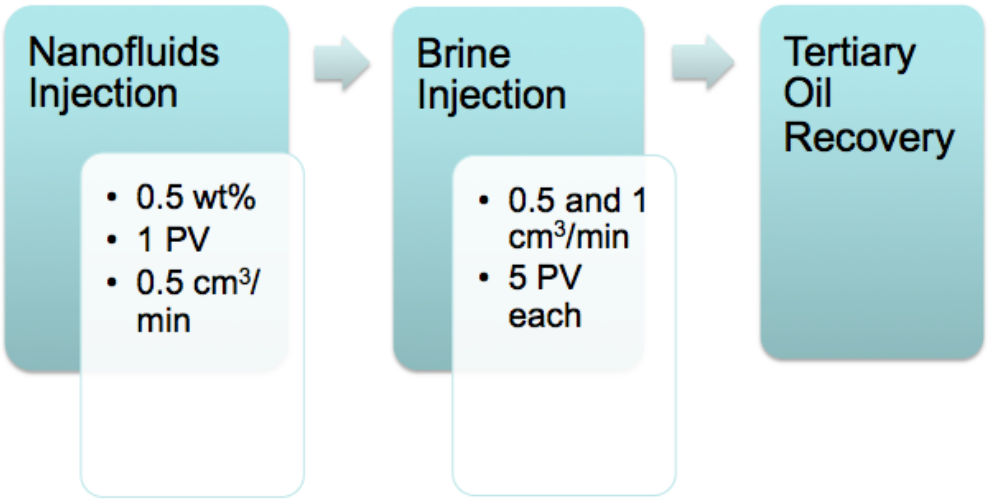

Figure 25. Procedure of the tertiary oil recovery process

4.4 Results and Discussion

4.4.1 Zeta Potential Measurements

The average value was +31.5 mV. The plus sign meant that the particles had positive charge. Since the value was larger than 30 mV, the suspension was stable enough to be used.

4.4.2 Coreflood Tests

The properties of the core calculated from the brine and oil saturation coreflood stages were given in **Table 7**.

Table 7 Core Descriptions

k, md	164.4
ϕ, %	12.84
PV, cm^3	22.31
S_{wi}, %	34.47
L, in	6.00
D, in	1.50
Weight Dry, g	381.11
Weight Saturated with Brine, g	404.10

Table 8 Secondary Recovery (Brine Injection) Results

Oil Recovery, cm^3	1.8
Residual Oil Volume, cm^3	12.82
S_{or}, %	57.4

At the secondary recovery stage, shown in **Table 8**, the residual oil saturation was still 57.4%. It meant the injection of brine only extracted 8% of the initial oil in place. Apparently, an enhanced oil recovery was required. **Figure 26** gave the relationship between the pressure drops across the core vs. the pore volume of brine injection during the secondary recovery. When the flow rate was constant, the permeability of the core did not change. As the flow rate increased, the pressure drop increased. It means that the permeability decreased as the flow rate increasing.

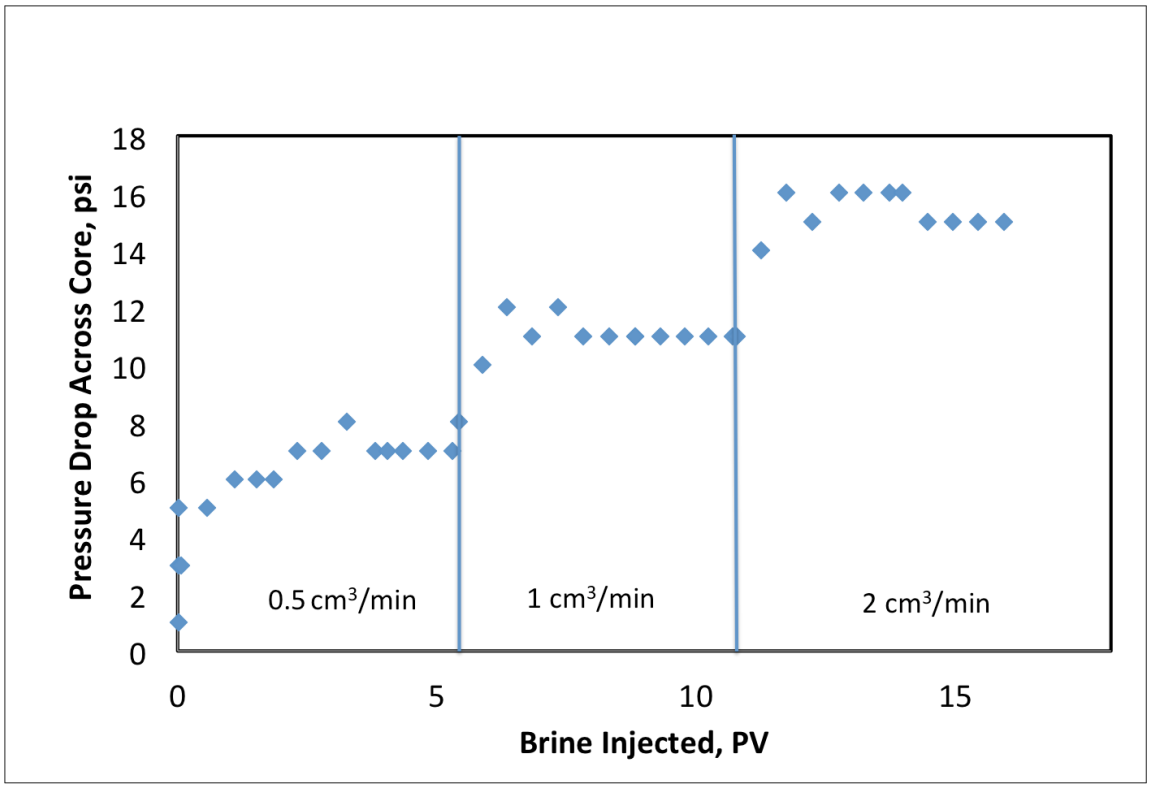

Figure 26. Pressure Drop vs. Pore Volume – Secondary Recovery

In the EOR process, flow rate was injected at both 0.5 cm^3/min and 1.0 cm^3/min. **Figure 27** showed that the permeability increased as we increase the injection rate, which is normal. The constant pressure drop during the time no flow rate was changed indicated that the experiment results were effective. No formation damage was created as the treatment was injected.

White residues were observed after the core was taken out. **Figure 28 (a)** was the photo of the inlet of the core. These white substances were believed as the nanoparticle suspensions of the treatment. After two days, flake-like solid formed all over the core as shown in **Figure 28 (b)**. The flake-like solid was the salt came out from the core. After

collecting the effluents, the total oil recovered in this stage was calculated. After the injection of the EOR agent and brine, 2 cm^3 oil was recovered. Since the OOIP was 14.62 cm^3 as calculated before, the tertiary recovery rate was 13.68%.

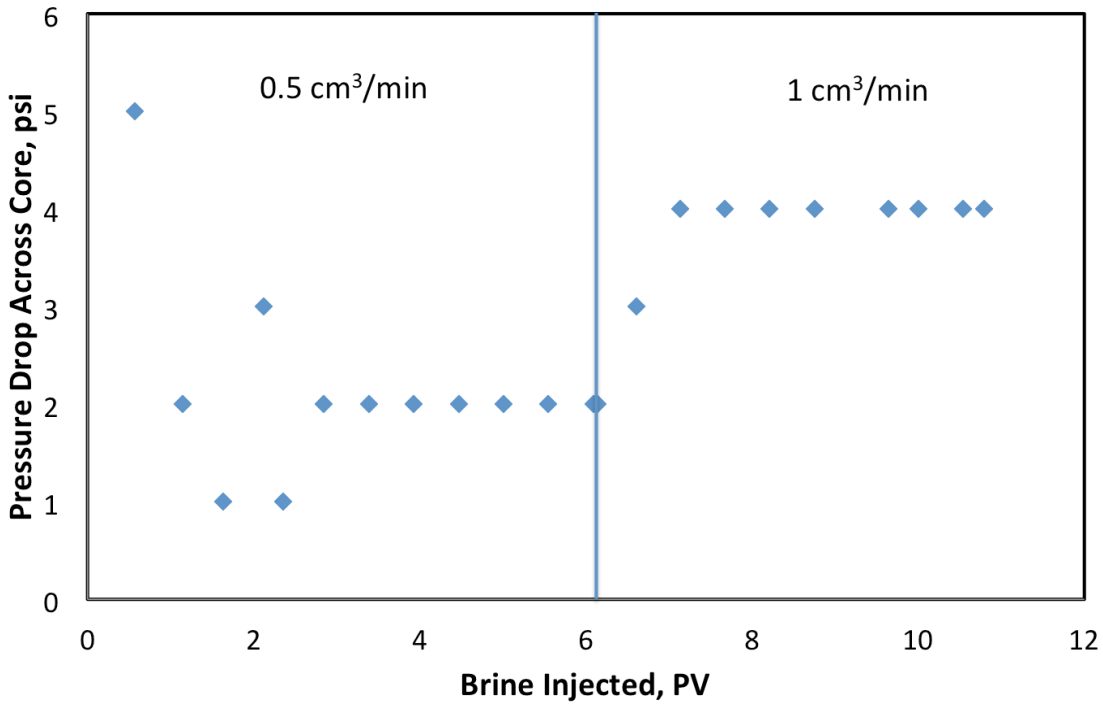

Figure 27. Pressure Drop vs. Pore Volume – Tertiary Recovery

(a) (b)

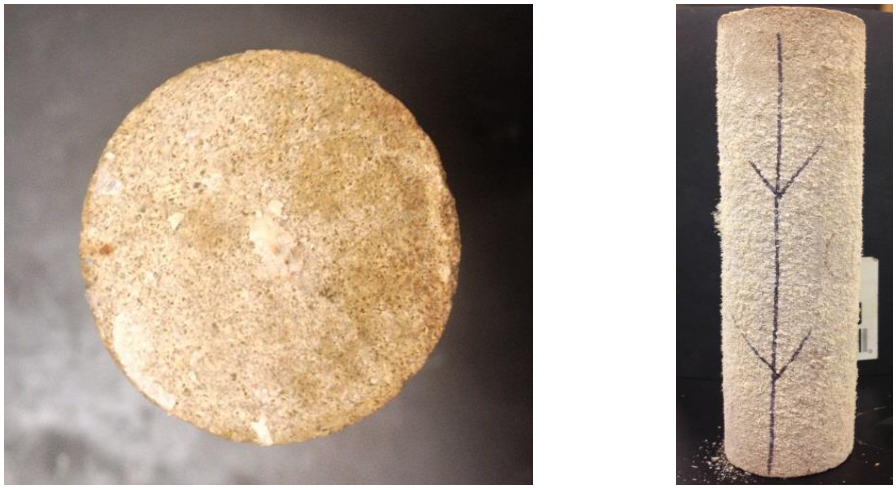

Figure 28. (a) White Residues at the Core Inlet (b) Flake-like Solid All over the Core

4.5 Conclusion

Alpha-phased zirconium phosphate suspension was used as an EOR agent to recovery dodecane in Indiana limestone core. The treatment was injected after the saturation of oil and the flooding of brine to get a tertiary recovery. The tertiary recovery rate was 13.68%, which proved that the treatment could be applied to recovery more oil.

5. CONCLUSIONS

Nanotechnology has already contributed significantly in many industries, such as electronics, materials, aerospace, biomedical and manufacturing. More recently, nanoparticles has been discussed as a new approach in many fields in oil and gas industry. This paper studied the usage of using alpha-phased zirconium phosphate nanofluids as a clay stabilizer and an EOR agent. By conducting coreflood experiments as well as testing the properties of the nanofluids, the following conclusions can be draw:

1. Both of the alpha-ZrP nanofluids modified with TBA and glucose gave shear-thinning performances. None of them were viscid enough to cause any formation damage.
2. Alpha-ZrP modified with glucose gave a lower surface tension than it modified with TBA. The α-ZrP-glucose had more potential to be used as an EOR agent than α-ZrP-TBA.
3. α-ZrP-glucose could worked as a clay stabilizer with Berea sandstone at high temperature (300°F) and high pressure (1000 psi).
4. A higher concentration may lead to a better result, however, if the concentration was too high (1.0 wt%), the pore throat would be blocked and more damages would occur.
5. 0.5 wt% α-ZrP-glucose diluted in 0.5 wt% of KCl solution was the best concentration of the treatment as clay stabilizer according to this study.

6. The alpha-ZrP emulsion could work as an EOR agent using Indiana limestone core and dodecane.
7. The tertiary recovery rate was 13.68%.

REFERENCES

B.A. Suleimanov, F.S.Ismailov, E.F. Veliyev. 2011. Nanofluid for Enhanced Oil Recovery. *Journal of Petroleum Science and Engineering* **78** (2): 431-437.

A. Haibi, M.A.H., H. Al-Hadrami, A. Al-Ajmi, Y. Al-Wahaibi, S. Ayatollahi. 2012. Effect of Mgo Nanofluid Injection into Water Sensitive Formation to Prevent the Water Shock Permeability Impariment. Paper presented at the SPE International Oilfield Nanotechnology Conference, Noordwijk, the Netherlands, 12-14 June. SPE-157106.

N.A. Ogolo, O.A.Olafuyi, M. O. Onyekonwu. 2013. Impact of Hydrocarbon on the Performance of Nanoparticles in Control of Fines Migration. Paper presented at the Nigeria Annual International Conference and Exhibition, Lagos, Nigeria, July 30 - August 1. SPE-167503.

I.A. El-Monier, H.A.Nasr-El-Din, T.L. Harper, R. Rosen. 2013. A New Environmentally Friendly Clay Stabilizer. *SPE Production & Operations* **28** (02): 145 - 153.

Z.J. Zhou, W.E.Gunter, R.G. Jonasson. 1995. Controlling Formation Damage Using Clay Stabilizers: A Review. Paper presented at the Annual Technical Meeting, Calgary, Alberta, June 7-9. PETSOC-95-71.

C. Belcher, K.S., R. Hollier, B. Paternostro. 2010. Maximizing Production Life with the Use of Nanotechnology to Prevent Fines Migration. Paper presented at the CPS/SPE International Oil & Gas Conference and Exhibition, Beijing, China, 8-10 June. SPE-132152.

T. Zhang, A.D., S.L. Bryant, C. Huh. 2010. Nanoparticle-Stabilized Emulsions for Applications in Enhanced Oil Recovery. Paper presented at the SPE Improved Oil Recovery Symposium Tulsa, Oklahoma, USA. 129885.

P.D. Nguyen, J.E.V., J.D. Weaver, T.D. Welton. 2010. Maintain Well Productivity through Inhibiting Scale Formation and Controlling Fines Migration. Paper presented at the SPE Asia Pacific Oil and Gas Conference and Exhibition, Bristane, Queensland, Australiz, 18-20 Dec. SPE-132663-MS.

B.G. Sharma, M.M.S. 1994. Polymerizable Ultra - Thin Films: A New Technique for Fines Stabilization. Paper presented at the SPE International Symposium on Formation Damage Control, Lafayette, Louisiana, 7-10 Feb. SPE-27345.

G.J. Ross. 1967. Kinetics of Acid Dissolution of an Orthochlorite Mineral *Canadian journal of chemistry* **45** (24): 3031-3034.

G.J. Ross. 1968. Structural Decomposition of an Orthochlorite During Its Acid Dissolution. *The Canadian Mineralogist* **9** (4): 522-530.

M.G. Reed. 1972. Stabilization of Formation Clays with Hydroxy-Aluminum Solutions. *Journal of Petroleum Technology* **24** (07): 860-864.

S.L. Berry, J.L.B., H.D. Bronnon. 2008. Performance Evaluation of Ionic Liquids as a Clay Stabilizer and Shale Inhibitor. Paper presented at the SPE International Symposium and Exhibition on Formation Damage Control, Lafayette, Louisiana, USA, 13-15 February. SPE-112540-MS.

T. Huang, J.B.C., J.R. Willingham. 2008. Using Nanoparticle Technology to Control Fine Migration. Paper presented at the SPE Annual Technical Conference and Exhibition, Denver, Colorado, USA, 21-24 September. SPE-115384-MS.

M. Ahmadi, A.H., P. Pourafshary, S. Ayatollahi. 2013. Zeta-Potential Investigation and Experimental Study of Nanoparticles Deposited on Rock Surface to Reduce Fines Migration *SPE Journal* **18** (03): 534-544. DOI: http://dx.doi.org/10.2118/142633-PA

N.A. Ogolo. 2013. The Trapping Capacity of Nanofluids on Migrating Fines in Sand. In *SPE Annual Technical Conference and Exhibition*. New Orleans, Louisiana, USA, 30 September - 2 October.

A.J.P. Fletcher, J.P.D. 2010. How Eor Can Be Transformed by Nanotechnology. Paper presented at the SPE Improved Oil Recovery Symposium, Tulsa, Oklahoma, USA, 24-28 April. SPE-129531.

S. Ayatollahi, M.M.Z. 2012. Nanotechnology-Assisted Eor Techniques: New Solutions to Old Challenges. Paper presented at the SPE International Oilfield Nanotechnology Conference, Noordwijk, The Netherlands, 12-14 June. SPE-157094.

S.K. Das, S.U.S.C., W. Yu, T. Pradeep. 2008. *Nanofluids Science and Technology*. hoboken, New Jersey: John Wiley & Sons, Inc. Original edition. ISBN 9780470074732.

D.T. Wasan, A.N., K. Kondiparty. 2011. The Wetting and Spreading of Nanofluids on Solids: Role of the Structural Disjoining Pressure. *Current Opinion in Colloid & Interface Science* **16** (4): 344-349.

L. Hendraningrat, B.E., S. Suwarno, O. Torsaeter. 2013. Laboratory Investigation of Permeability and Porosity Impairments in Berea Sandstone Due to Hydrophilic Nanoparticles Retention. Paper presented at the International conference on Geotechnical Engineering, Hammamet, Tunisia, 21-23 February. Paper W0182.

A.F. Mejia, A.D., S. Pullela, Y. Chang, M. Simonetty, C. Carpenter, J.D. Batteas, M.S. Mannan, A. Clearfield, Z. Cheng. 2012. Pickering Emulsions Stabilizedn by Amphiphilic Nano-Sheets. *Soft Matter* **8**: 10245-10253. DOI: 10.1039/c2sm25846c

X. Kong, M.M.O. 2010. Application of Micro and Nano Technologies in the Oil and Gas Industry - an Overview of the Recent Progress. Paper presented at the Abu Dhabi International Petroleum Exhibition & Conference, Abu Dhabi, UAE, 1-4 November. SPE-138241.